Shaping a time-dependent excitation to minimize the shot noise in a tunnel junction

Julien Gabelli[1] and Bertrand Reulet[1,2]

[1]*Laboratoire de Physique des Solides, Univ. Paris-Sud, CNRS, UMR 8502, F-91405 Orsay Cedex, France*

[2]*Université de Sherbrooke, Sherbrooke, Québec J1K 2R1, Canada*

(Received 16 May 2012; published 4 February 2013)

We report measurements of shot noise in a tunnel junction under biharmonic illumination, $V_{ac}(t) = V_{ac1}\cos(2\pi\nu t) + V_{ac2}\cos(4\pi\nu t + \varphi)$. The experiment is performed in the quantum regime, $h\nu \gg k_B T$ at low temperature $T = 70$ mK and high frequency $\nu = 10$ GHz. From the measurement of noise at low frequency, we show that we can infer and control the nonequilibrium electronic distribution function by adjusting the amplitudes and phase of the excitation, thus modeling its shape. In particular, we observe that the noise depends not only on the amplitude of the two sine waves but also on their relative phase, due to coherent emission/absorption of photons at different frequencies. By shaping the excitation we can minimize the noise of the junction, which no longer reaches its minimum at zero dc bias. We show that adding an excitation at frequency 2ν with the proper amplitude and phase can *reduce* the noise of the junction excited at frequency ν only.

DOI: 10.1103/PhysRevB.87.075403 PACS number(s): 72.70.+m, 05.40.−a, 42.50.Lc, 73.23.−b

I. INTRODUCTION

In recent years the dynamical control of mesoscopic conductors has gained increasing interest, mainly motivated by the realization of phase-coherent electronics for quantum computation. One major challenge is the experimental achievement of a single electron excitation above the Fermi sea. The way to drive the ground state of a metallic conductor to reach the single electron excitation should be optimized to minimize the creation of electron-hole excitations; this can be probed by noise measurements.[1–7] For a conductor with energy-independent transmission, the variance of the current fluctuations due to the discrete nature of electrons, the so-called shot noise, reaches a minimum when the excitation $V_L(t)$ is a $T = 1/\nu$ periodic sequence of Lorentzian peaks of quantized area $\int_0^T eV_L(t)\,dt = Nh$ each, with N integer. In a tunnel junction this leads to a noise spectral density $S_2 = Ne^2\nu$, i.e., the same as the shot noise of a purely dc current $I = Ne\nu$. Thus, this ac excitation creates a nonequilibrium electron distribution function with the remarkable property that it yields to a charge transfer of N electrons per cycle in average with a variance $\Delta N^2 = N$.

It is experimentally difficult to generate Lorentzian pulses with precise shape and high repetition rate, a condition necessary to observe the predictions.[1,2] The simplest ac excitation consists of a pure sine wave $V_{ac}\cos(2\pi\nu t)$. Unfortunately, the presence of the ac voltage always increases the noise,[8–11] i.e., $S_2(V_{dc}, V_{ac}) > S_2(V_{dc}, V_{ac} = 0)$, where S_2 is the noise spectral density measured at low frequency. A much richer waveform, which we have used in the present work, is the biharmonic excitation:

$$V_{ac}(t) = V_{ac1}\cos(2\pi\nu t) + V_{ac2}\cos(4\pi\nu t + \varphi). \qquad (1)$$

By controlling the three parameters $V_{ac1}, V_{ac2}, \varphi$, one can modify the shape of the ac excitation, which modifies the out-of-equilibrium electron distribution function and thus the noise. As we show below, adding the excitation at frequency 2ν may lower the noise, i.e., $S_2(V_{dc}, V_{ac1}, V_{ac2}) < S_2(V_{dc}, V_{ac1}, V_{ac2} = 0)$, thus partially erasing the extra noise created by the excitation at frequency ν. This occurs because the absorption/emission of two photons of frequency ν may interfere destructively with that of one photon of frequency 2ν.

The paper is organized as follows. In Sec. II, we describe the experimental setup. In Sec. III, we calculate the nonequilibrium stationary distribution function generated by any time-dependent, periodic excitation. From the noise measurements we deduce in Sec. IV the experimental electron distribution function in the presence of the biharmonic excitation. We show in Sec. V that a biharmonic excitation with two spectral components ν and 2ν can reduce the monoharmonic photon-assisted noise at frequency ν. In Sec. VI, we summarize our discussion. For the sake of clarity, some technical details are moved from the main body of the paper to the Appendices.

II. EXPERIMENTAL SETUP

We have measured the shot noise of an Al/Al oxide/Al tunnel junction similar to that used for noise thermometry[12] cooled to 70 mK. We apply a 0.1 T perpendicular magnetic field to turn the Al normal. We measure the noise at low frequency while the junction is excited by the biharmonic ac voltage (1), as depicted in Fig. 1. To generate the biharmonic signal, a microwave source of frequency $\nu = 10$ GHz is split in two arms. A frequency doubler in the upper arm generates the oscillating voltage at $2\nu = 20$ GHz. Its phase φ can be tuned by a mechanical phase shifter while its amplitude V_{ac2} is set by the tunable output power of the source. In the lower arm, a variable attenuator allows us to modify V_{ac1}. The signals from the two arms are recombined at point A and sent to the sample through a directional coupler placed at liquid helium temperature. A bias tee, sketched by an inductor and a capacitor in Fig. 1, allows us to add the dc voltage V_{dc} to the ac one coming from the coupler. An example of an achievable waveform is shown in Fig. 1(b), together with a Lorentzian. The ac voltages experienced by the sample are measured by fitting the data of the photo-assisted noise with a single frequency, as in Ref. 11. The resistance of the sample $1/G = 48\ \Omega$ is close enough to 50 Ω to provide a good impedance matching to the coaxial cable and avoid reflection of the ac excitation. Thus, only the fluctuating current due to the tunneling process is amplified by a low noise cryogenic amplifier (noise temperature

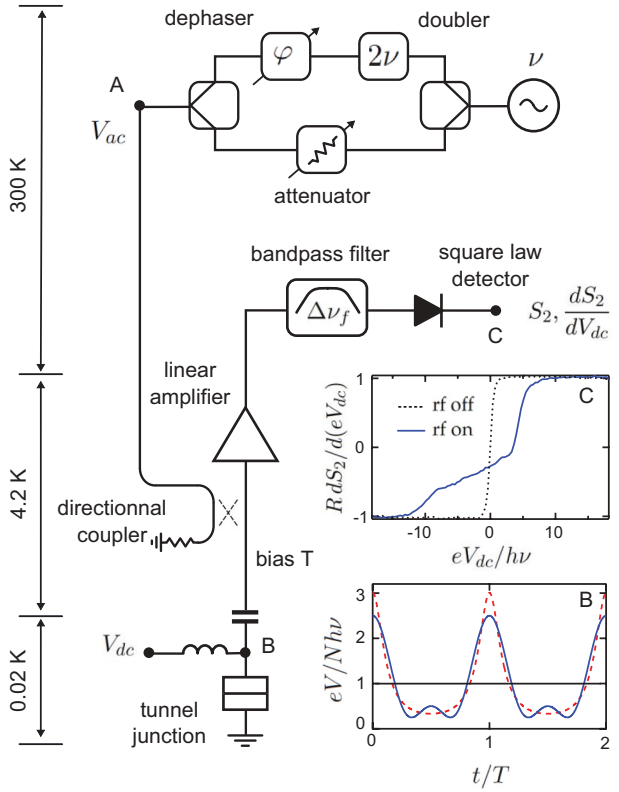

FIG. 1. (Color online) Experimental setup for the measurement of the photon-assisted noise in a tunnel junction under biharmonic excitation. Inset B: T-periodic sequence of biharmonic excitation (blue line) with $eV_{dc} = eV_{ac1} = 2eV_{ac2} = h\nu$ and $\varphi = 0$, approximating Lorentzian pulses of width $\tau = \ln 2/(2\pi\ T)$ and height $N = 1$ (red dashed line). Inset C: normalized differential noise spectral density with (blue line) and without (black dotted line) microwave excitation vs normalized dc bias. The power of the generator, the variable attenuator, and the phase shifter are tuned to obtain $eV_{ac1} = 2eV_{ac2} = 5.4\ h\nu$ and $\varphi = 0$.

$T_N \simeq 7$ K). The noise is filtered to keep frequencies in the range 0.5–1.8 GHz before impinging on a power detector. The dc voltage at point C is proportional to the noise power density S_2 integrated over the bandwidth of the filter, see Appendix A. The derivative of the noise $\partial S_2/\partial eV_{dc}$ is measured with an additional 77 Hz, small voltage modulation, and a usual lock-in detection. To calibrate the measurement, we use the noise spectral density at high voltage being $S_2(eV \gg k_BT) = eI$ as in shot noise thermometry.[12] Figure 1(c) shows measurements of the differential noise $\partial S_2/\partial eV_{dc}$ with and without ac excitation. From the data without ac excitation and taking into account the finite bandwidth of the detection, we determine the electrons temperature: $T_{el} = 70$ mK $= 0.14\ h\nu/k_B$. When the ac excitation is switched on, the differential noise exhibits an intermediate step, a consequence of the electron energy distribution function differing from that of Fermi-Dirac.

III. MEASUREMENTS OF DISTRIBUTION FUNCTIONS

Distribution functions in samples driven out of equilibrium by a dc voltage have been obtained by the measurement of the differential conductance in systems where the density of states depends on energy. This occurs with superconducting electrodes,[13,14] in the presence of dynamical Coulomb blockade[15,16] or with a quantum dot.[17] In our case, the differential conductance of the junction is totally voltage-independent and its measurement does not provide any spectroscopic information. However, as we show below, the differential noise does. As with differential conductance measurements, we cannot access the distribution functions of the two contacts separately. We measure the distribution functions that are involved in the transport, which depends only on the voltage difference between the contacts. This can be described by taking one of the contacts at equilibrium while the other one experiences the full time-dependent voltage. For not too small energy ξ, $\xi \gg h\Delta\nu_f, k_BT_{el}$ where $\Delta\nu_f = 1.3$ GHz is the bandwidth of the noise detection, we show in Appendix A that the distribution function $\tilde{f}$ is related to the differential noise $\partial S_2/\partial eV_{dc}$ by

$$\tilde{f}(\epsilon_F + \xi) \simeq \frac{1}{2}\left(1 - \frac{1}{G}\frac{\partial S_2}{\partial eV_{dc}}\right)_{eV_{dc}=\xi}. \tag{2}$$

An energy resolution better than $h\Delta\nu, k_BT_{el}$ can be achieved by numerical deconvolution of the noise data, as explained in Appendix A.

IV. DISTRIBUTION FUNCTION FOR A TIME-DEPENDENT EXCITATION

In the presence of a periodic voltage $V_{ac}(t)$ of frequency ν, the electron wave functions acquire an extra phase factor:[19]

$$\Xi(t) = \exp\left(\frac{-i}{\hbar}\int_0^t eV_{ac}(t')\,dt'\right). \tag{3}$$

Electronic states with energy ϵ are split into subbands with energies $\epsilon \pm nh\nu$ and spectral weight given by the modulus squared of the Fourier coefficients c_n of $\Xi(t) = \sum_{n=-\infty}^{+\infty} c_n e^{i2\pi\nu nt}$. The corresponding nonequilibrium distribution function is[20]

$$\tilde{f}(\epsilon) = \sum_{n=-\infty}^{+\infty} |c_n|^2 f(\epsilon + nh\nu), \tag{4}$$

where f is the equilibrium Fermi-Dirac distribution. For harmonic excitation ($V_{ac2} = 0$), $c_n = J_n(eV_{ac1}/h\nu)$ with J_n the Bessel functions of the first kind. For biharmonic excitation:

$$c_n = \sum_{m=-\infty}^{+\infty} J_{n-2m}\left(\frac{eV_{ac1}}{h\nu}\right) J_m\left(\frac{eV_{ac2}}{2h\nu}\right) e^{-im\varphi}. \tag{5}$$

The sum in Eq. (5) expresses the interference involving several absorption/emission processes of photons of frequencies ν and 2ν. This interference depends on the relative phase φ. Figure 2 shows measured nonequilibrium distribution functions $\tilde{f}$ for different ac excitations. They are obtained from numerical deconvolution of the noise data (see Appendix A). Although biharmonic excitation depends on only three parameters V_{ac1}, V_{ac2}, and φ, a large class of distribution functions can be realized, which allows us to control related physical properties such as the shot noise. For example, taking $V_{ac1} = 2V_{ac2}$ creates a distribution function with two steps. The height and width of the steps can be controlled by tuning the phase shift [see Fig. 2(a)] or the amplitude of the ac excitation [see Figs. 2(b)–2(c)]. We show in the following that this

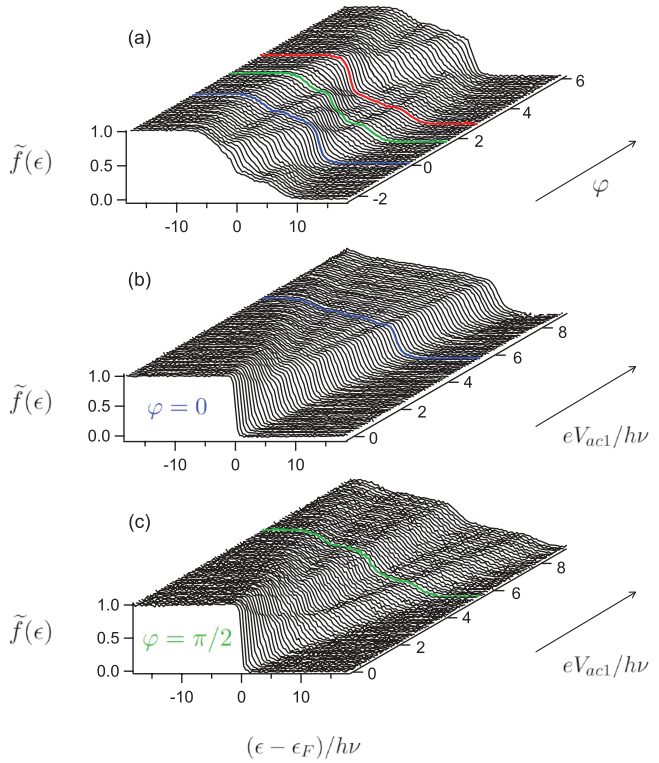

FIG. 2. (Color online) Nonequilibrium distribution functions obtained from numerical deconvolution of the measured differential noise. (a) Noise is measured for $eV_{ac1} = 2eV_{ac2} = 5.4\ h\nu$, for phase shifts $\varphi = 0$ (blue), $\varphi = \pi/2$ (green), and $\varphi = \pi$ (red). (b) [resp. (c)] Noise is measured for various amplitudes of excitation V_{ac1} and V_{ac2} keeping $V_{ac1} = 2V_{ac2}$, for $\varphi = 0$ (resp. $\varphi = \pi/2$).

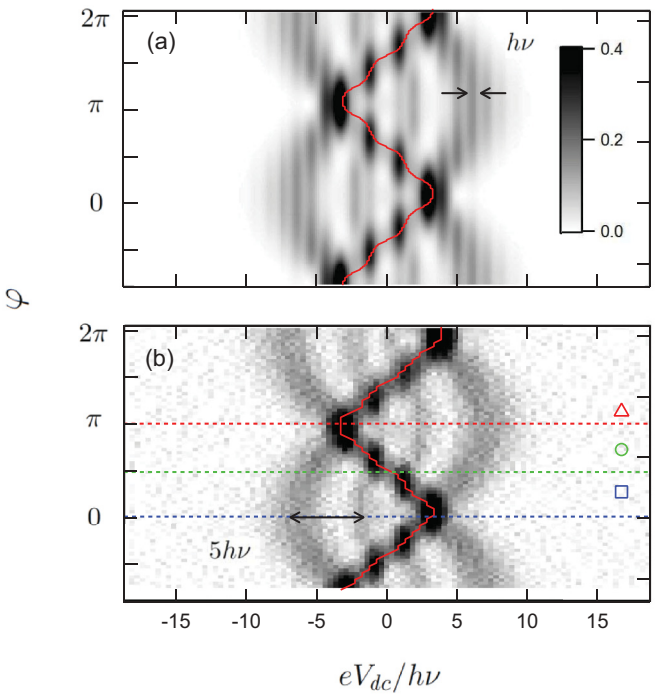

FIG. 3. (Color online) Calculated (a) and measured (b) second derivative of the biharmonic photon-assisted noise $\partial^2 S_{2,ac}/\partial V_{dc}^2$ as a function of normalized dc bias and phase shift. In both cases $eV_{ac1} = 2eV_{ac2} = 5.4\ h\nu$ with $\nu = 10$ GHz, and the temperature is $T_{el} = 0.14\, h\nu/k_B = 70$ mK. Red curves correspond to the calculated (a) and measured (b) minimum of the photon-assisted noise, $\partial S_{2,ac}/\partial V_{dc} = 0$. Dashed lines correspond to phase shifts that are used in Fig. 4.

distribution minimizes the shot noise for a given amplitude V_{ac1}. Making the spectroscopy of a system with discrete levels has been performed in solid state qubits with harmonic[21] and biharmonic[22] excitation. In such systems, one can directly measure the population of the levels in the presence of the excitation. In our case, the noise, i.e., the variance of the fluctuations of the populations, provides the spectroscopic information. It should be noted that the energy distribution function $\tilde{f}(\epsilon)$ refers to a single-particle distribution function and takes, by definition, no account of potential correlations between electrons and holes.

V. NOISE MINIMIZATION

In the following we show how controlling the distribution function via the shape of the exciting waveform allows us to reduce the shot noise in the tunnel junction. The current noise of a coherent conductor biased by a time-dependent, periodic voltage has been calculated for a pure sine wave excitation.[8,23] For a tunnel junction and an arbitrary periodic excitation, we obtain

$$S_{2,ac}(eV_{dc}) = \sum_{n=-\infty}^{+\infty} |c_n|^2\, S_2^{(0)}(eV_{dc} + nh\nu), \qquad (6)$$

where $S_2^{(0)}(h\nu) = Gh\nu \coth(h\nu/2k_BT_{el})$ is the Johnson-Nyquist equilibrium noise, and c_n are given by Eq. (5). In the case of a harmonic excitation, one observes features on $S_{2,ac}(eV_{dc})$ at bias $eV_{dc} = nh\nu$ with n integer (discontinuities of dS_2/dV rounded by the finite temperature and detection bandwidth).[9,11] For biharmonic excitation the interferences between multi-photon-assisted processes at frequency ν and 2ν induce interference fringes on a larger scale. We show this additional complexity in the interference pattern for $V_{ac1} = 2V_{ac2}$ in Fig. 3(b), where the second derivative of the noise $\partial^2 S_{2,ac}/\partial eV_{dc}^2$ is plotted. The choice $V_{ac1} = 2V_{ac2}$ has been motivated by a numerical calculation described in Appendix B. The interference pattern in the (eV_{dc},φ) space exhibits fringes with a fringe spacing $\simeq 5h\nu$ [see Fig. 3(b)], in agreement with numerical calculations using Eqs. (5) and (6), see Fig. 3(a), whereas the substructure at $h\nu$ is almost washed out by thermal broadening. Red curves in Fig. 3 correspond to the calculated (a) and measured (b) eV_{dc} value at which the photon-assisted noise is minimal ($\partial S_{2,ac}/\partial eV_{dc} = 0$). It exhibits steps at $eV_{dc} = \pm h\nu$ and $eV_{dc} = \pm 3h\nu$.

The appearance of fringes at a scale larger than $h\nu$ is similar to what is observed when systems with discrete spectrum are driven by a large amplitude signal:[21,24] The fringes due to individual photon resonances, characterized by the energy scale $h\nu$, are superimposed fringes with larger characteristic scale corresponding to Stückelberg oscillations. The latter may persist even if the $h\nu$ pattern is lost and are a direct consequence of quantum coherence. In our case, two contacts with time-dependent chemical potentials are coupled by tunneling. The phase acquired by the electron-hole

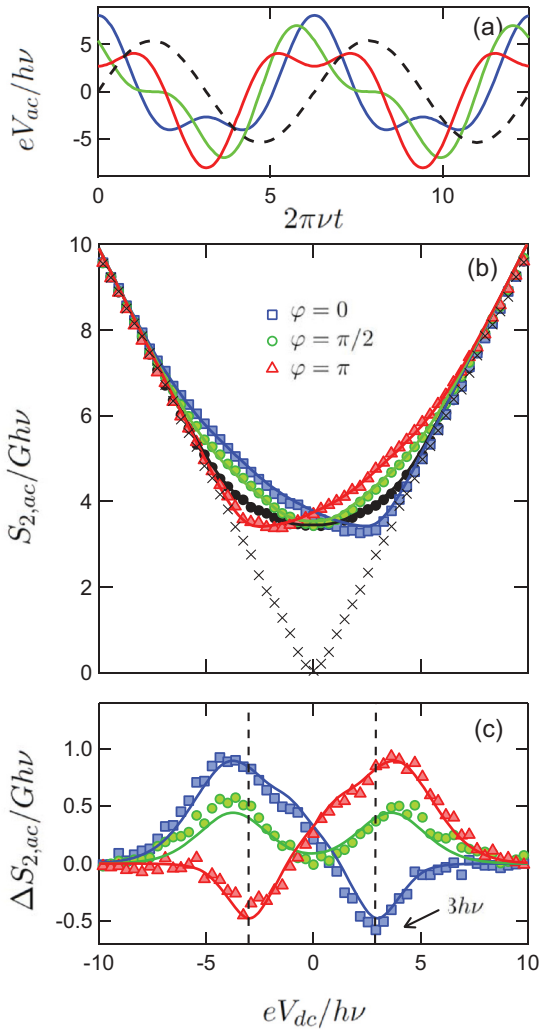

FIG. 4. (Color online) (a) Shape of the ac excitation with the different phase shifts: $\varphi = 0$ (blue), $\varphi = \pi/2$ (green) and $\varphi = \pi$ (red). Dashed line: monoharmonic signal. (b) Normalized biharmonic photon-assisted noise $S_{2,ac}/Gh\nu$ vs normalized dc bias for $eV_{ac1} = 5.4h\nu$. Blue square, green circle, red triangle symbols: data for $eV_{ac2} = 2.7h\nu$ and phase shifts $\varphi = 0,\pi/2,\pi$. Black circles: data for $V_{ac2} = 0$, i.e., pure sine wave excitation. Cross symbols ($\times$): data for $V_{ac1} = V_{ac2} = 0$, i.e., shot noise without any ac excitation. Solid lines: theoretical predictions, Eqs. (5) and (6). (c) Difference between biharmonic and monoharmonic photon-assisted noise $\Delta S_{2,ac}(V_{dc}) = S_{2,ac}(V_{dc},V_{ac1},V_{ac2}) - S_{2,ac}(V_{dc},V_{ac1},V_{ac2} = 0)$.

pairs involved in the transport mechanism depends on the time dependence of the voltage. The probability to cross the barrier involves interferences between several processes, which results in the Stückelberg-like oscillations we observe.[25] This behavior is generic for driven quantum systems and is a part of the more general effect of Ramsey multiple-time-slit interferences.[26]

We have calculated numerically the set of parameters $(eV_{dc},eV_{ac2},\varphi)$ minimizing the photon-assisted noise $S_{2,ac}$ for a given eV_{ac1} and temperature T_{el}, see Appendix B. The optimal dc voltage is zero only for $\varphi = \pi/2$, which corresponds to the existence of a symmetry in the waveform: For each positive value of $V_{ac}(t)$ there is a symmetric, negative value [green curve on Fig. 4(a)]. When this symmetry is lost there is no reason for the noise to reach its minimum at $V_{dc} = 0$. For experimental parameters $T = 0.14\ h\nu/k_B$ and $eV_{ac1} = 5.4\ h\nu$, we obtain that optimal values are $eV_{ac2} = eV_{dc} = 2.4\ h\nu$ and $\varphi = 0$. For $\varphi = \pi$, the waveform is reversed [see Fig. 4(a)] and the minimum occurs at the opposite value of V_{dc}. Figure 4(b) shows noise measured for $eV_{ac2} = 2.7\ h\nu$ (i.e., close to optimal) for $\varphi = 0$ (blue), $\pi/2$ (green), and π (red). All the data (symbols) are very well fitted by the theory (solid lines). One observes that the minima for $\varphi = 0$ and π occur at opposite values of $eV_{dc} = \pm 2.3\ h\nu$ in agreement with the numerical result.

The black curve on Fig. 4(b) (black circles) shows the noise for $V_{ac2} = 0$. There is a clear region of V_{dc} where it is *above* the red or blue curve, which correspond to $V_{ac2} \neq 0$. We have emphasized this result by plotting in Fig. 4(c) the difference $\Delta S_{2,ac}(V_{dc}) = S_{2,ac}(V_{dc},V_{ac1},V_{ac2}) - S_{2,ac}(V_{dc},V_{ac1},V_{ac2} = 0)$ between the noise under biharmonic and monoharmonic excitations, which can be negative. This proves that the addition of the excitation at frequency 2ν may *reduce* the noise. It is also noticeable that the noise under biharmonic excitations drops *below the absolute minimum* of the noise with monoharmonic excitation, which occurs at zero bias, in agreement with our numerical simulations (see Appendix B).

Noise has been predicted to be minimal when the excitation is a sequence of Lorentzian peaks of a quantized area $\int_0^T eV(t)\,dt = Nh$.[1,2] Such an excitation does not add more noise than its dc voltage alone. In other words, the noise as a function of the dc voltage has minima for quantized values of V_{dc}. This property seems to be valid for many ac waveforms at zero temperature,[6] including the biharmonic excitation (see Appendix C). We observe that this is no longer the case at finite temperature for the biharmonic excitation (data not shown), in agreement with numerical calculations (see Appendix C). Let us now consider the difference in the noise for two excitations at the same frequency. Obviously, it should have extrema for the same quantized values of V_{dc} at zero temperature. As shown in Fig. 4(c), this property seems to survive at finite temperature if we consider the difference between the monoharmonic and biharmonic excitations $\Delta S_{2,ac}$, which has minima at $\pm 3h\nu$.

VI. CONCLUSION

We have observed the effect of biharmonic illumination on the nonequilibrium current noise in a tunnel junction. We have measured the low frequency shot noise of the junction while varying the shape of the ac excitation and showed that from these measurements we can determine the out-of-equilibrium distribution function induced by the excitation. This opens the way of engineering the waveform of an ac signal to control the out-of-equilibrium distribution function of the electrons in a mesoscopic conductor, thus modifying its physical properties. We have demonstrated this ability by reducing the shot noise in a tunnel junction irradiated at frequency ν by adding another coherent irradiation at frequency 2ν of controlled amplitude and phase. Such a procedure may be used in many situations. For example, it may be used to dynamically control the amplitude of the critical current of a superconductor/normal metal/superconductor tunnel junction,[27] or even reverse it as

with a dc current.[28,29] This would realize a Josephson junction that can be switched from 0 state to π state dynamically, an interesting device in the context of quantum computation.

ACKNOWLEDGMENTS

We are very grateful to Lafe Spietz for providing us with the sample and to Leonid Levitov for many stimulating discussions. We thank Marco Aprili, Wolfgang Belzig, Sophie Guéron, and Mihajlo Vanevic for fruitful discussions. This work was supported by ANR-11-JS04-006-01 and the Canada Excellence Research Chair program.

APPENDIX A: TUNNELING SPECTROSCOPY OF DISTRIBUTION FUNCTIONS

The quantity we measure is

$$\Delta I^2(eV_{dc}) = \int_{-\infty}^{+\infty} S_2(eV_{dc},h\nu')\,|H(\nu')|^2\,d\nu', \qquad \text{(A1)}$$

where $S_2(eV_{dc},h\nu')$ is the spectral density of current fluctuations at frequency ν' and $H(\nu')$ the frequency response of the bandpass filter, of width $\Delta\nu_f$, and central frequency ν_f (in our experiment, $\nu_f = 1.15$ GHz, $\Delta\nu_f = 1.3$ GHz). $S_2(eV_{dc},h\nu')$ depends on the ac excitation $V_{ac}(t)$. For a tunnel junction with energy-independent transmissions, $S_2(eV_{dc},h\nu')$ is simply

$$S_2(eV_{dc},h\nu') = \tfrac{1}{2}\big[S_2^{(0)}(eV_{dc}+h\nu') + S_2^{(0)}(eV_{dc}-h\nu')\big], \qquad \text{(A2)}$$

with $S_2^{(0)}(eV_{dc}) = S_2(eV_{dc},0)$ the zero-frequency noise spectral density, given by

$$S_2^{(0)}(eV_{dc}) = G\int_{-\infty}^{+\infty}[f_L(\epsilon)(1-f_R(\epsilon)) + f_R(\epsilon)(1-f_L(\epsilon))]\,d\epsilon. \qquad \text{(A3)}$$

Here f_L (respectively f_R) is the energy distribution function of electrons in the left (resp. right) contact. In the presence of both dc and ac bias, we can without loss of generality consider that the dc bias is applied to the left reservoir while the ac voltage is applied to the right one. Thus f_L is the Fermi-Dirac distribution f with a shifted electrochemical potential, $f_L(\epsilon) = f(\epsilon - eV_{dc})$, whereas $f_R = \tilde{f}$ is the nonequilibrium distribution function we wish to measure. Defining the difference in the noise with and without ac excitation, $M(eV_{dc}) = \Delta I^2(eV_{dc},eV_{ac}\neq 0) - \Delta I^2(eV_{dc},eV_{ac}=0)$, we obtain the following convolution:

$$\frac{\partial M}{\partial eV_{dc}}(eV_{dc}) = \int_{-\infty}^{+\infty} K(eV_{dc}-\epsilon)\,[\tilde{f}(\epsilon)-f(\epsilon)]\,d\epsilon \qquad \text{(A4)}$$

with a kernel:

$$K(\epsilon) = -\frac{G}{h}\int_{-\infty}^{+\infty}|H(\nu')|^2\,\frac{\partial f}{\partial\nu'}(h\nu'-\epsilon)\,d\nu'. \qquad \text{(A5)}$$

Thus, the nonequilibrium function $\tilde{f}$ can be calculated using the Fourier transform FT:

$$\tilde{f}(\epsilon) = f(\epsilon) + FT^{-1}\left\{\frac{FT\left[\frac{\partial M}{\partial eV_{dc}}\right]}{FT[K]}\right\}(\epsilon). \qquad \text{(A6)}$$

In the limit $\xi \gg h\nu_F, h\Delta\nu_f, k_BT_{el}$, using $K(\epsilon) = -4G\Delta\nu_f\,\delta(\epsilon-\epsilon_F)$, Eq. (A6) reduces to

$$\tilde{f}(\epsilon_F+\xi) \simeq \frac{1}{2}\left(1-\frac{1}{G}\frac{\partial S_2}{\partial eV_{dc}}\right)_{eV_{dc}=\xi}. \qquad \text{(A7)}$$

In our experiment, $h\nu_f/k_B = 50$ mK, $h\Delta\nu_f/k_B = 56$ mK, and $T_{el} = 70$ mK.

APPENDIX B: OPTIMIZATION OF THE BIHARMONIC PHOTON-ASSISTED NOISE AT FINITE TEMPERATURE

The photon-assisted noise in the tunnel junction depends on the shape of the ac excitation. In the case of biharmonic excitation, we determine numerically the set of parameters $(eV_{dc}^\star, eV_{ac1}^\star, eV_{ac2}^\star, \varphi^\star)$ which minimize the noise at temperature T_{el}. At each temperature, the noise spectral density is calculated for $100\times100\times100\times100$ different values of $(eV_{dc}/h\nu, eV_{ac1}/h\nu, eV_{ac2}/h\nu, \varphi)$ in the range $[-5,5]\times[0,10]\times[0,5]\times[0,\pi]$. Let us suppose we excite at frequency ν with an amplitude V_{ac1} and we want to minimize the low frequency shot noise. Figures 5(a) and 5(b) show respectively how to choose V_{dc} and V_{ac2} to reach this goal, as a function of V_{ac1} and for various T_{el}. The obtained noise reduction, $R = S_2(V_{dc}=0,V_{ac1},V_{ac2}=0) - S_2(V_{dc}^\star,V_{ac1},V_{ac2}^\star)$, is plotted in Fig. 5(c). It appears that one always has $V_{dc}^\star \simeq V_{ac2}^\star$. For example, for our experimental parameters $k_BT_{el} = 0.14\ h\nu$ and $eV_{ac1} = 5.4\ h\nu$, the optimum is $eV_{dc} = 2.38\ h\nu$, $eV_{ac2} = 2.4\ h\nu$, and $\varphi = 0$ (or the opposite V_{dc} for $\varphi = \pi$). Adding dc voltage and ac voltage at frequency 2ν allows us to reduce the noise below that with no dc bias and the same excitation at frequency ν, by an amount $R = 0.04\ Gh\nu$ (or in terms of noise temperature, by 20 mK). We observe this effect in Fig. 4(b) of the paper: The minimum of $S_2(V_{dc},V_{ac1},V_{ac2}^\star)$ drops below $S_2(V_{dc}=0,V_{ac1},V_{ac2}=0)$ for $V_{dc}\sim V_{dc}^\star$.

For a given V_{ac1}, there is a temperature $T_{\max}(eV_{ac_1})$ above which the optimal point does not exist anymore: $V_{dc}^\star = V_{ac2}^\star = 0$, see inset of Fig. 5(c). Above that temperature, adding a second harmonic will never reduce the noise. In particular, for $eV_{ac1} < 2\ h\nu$ it is never possible to reduce the noise with a biharmonic excitation. In our experiment, $T_{\max}\simeq 250$ mK $> T_{el}$, so the addition of the sine wave at frequency 2ν may lead to a reduction of the noise, as we observe.

It is interesting to remark that the waveform we found that minimizes the noise for a given V_{ac1} at finite temperature is not close to Lorentzian, but corresponds almost to the first two harmonics of a Lorentzian with a dc offset [see Fig. 1(b)]. The Lorentzian pulses are optimal only if we consider the noise at zero frequency, zero temperature, and integer values of $eV_{dc}/h\nu$. They are no longer optimal if we work at finite detection frequency, finite temperature, or a noninteger value of $eV_{dc}/h\nu$, see Appendix C.

APPENDIX C: PHOTON-ASSISTED NOISE AT FINITE TEMPERATURE FOR VARIOUS WAVEFORMS

We consider the three waveforms shown in Fig. 6(a): $V_L(t)$ is the Lorentzian shape of width $\tau = \ln 2/2\pi\ T$ (this value is chosen to have the same first two harmonics as the one we have chosen in our experiment), $V_1(t) = V_{dc}[1+\cos(2\pi\nu t)]$ is the same Lorentzian waveform truncated to the same dc and first

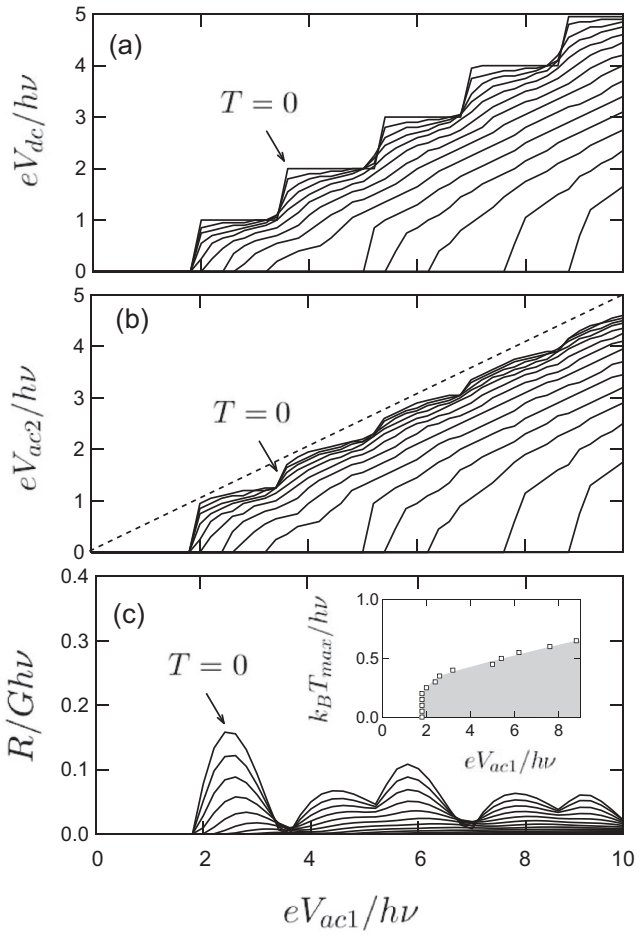

FIG. 5. (a) Optimal value of the reduced dc voltage $eV_{dc}/h\nu$. Optimal value of the reduced amplitude $eV_{ac2}/h\nu$ at frequency 2ν. (c): Noise reduction $R = S_2(V_{dc} = 0, V_{ac1}, V_{ac2} = 0) - S_2(V^\star_{dc}, V_{ac1}, V^\star_{ac2})$ between the monoharmonic photon-assisted noise at zero dc bias and the optimal biharmonic one with the same ac amplitude V_{ac1} at frequency ν. (a), (b), and (c) are plotted as a function of the reduced amplitude $eV_{ac1}/h\nu$ at frequency ν, for various reduced temperature $k_BT_{el}/h\nu$ ranging from 0 (blue line) to 0.65 by steps of 0.05. Inset: Temperature above which the noise cannot be reduced by biharmonic excitation.

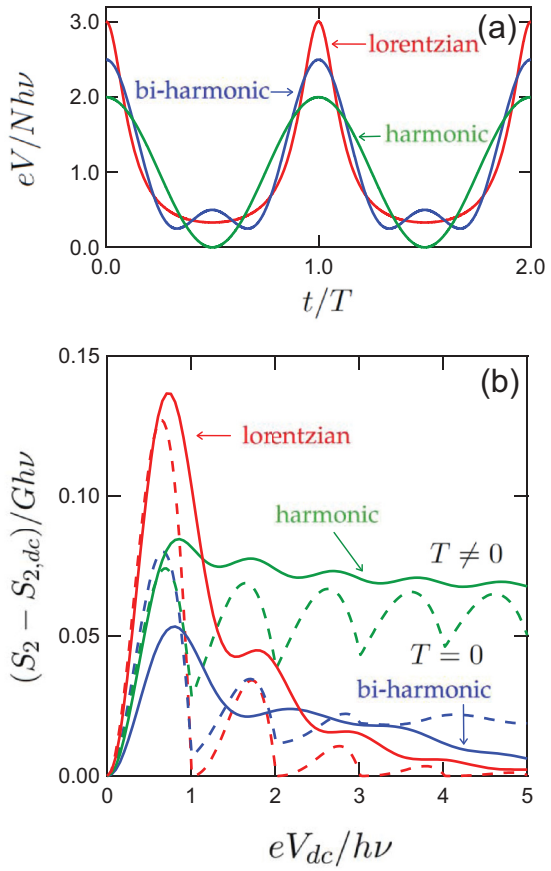

FIG. 6. (Color online) (a) T-periodic sequence of Lorentzian pulses of width $\tau = \ln 2/2\pi\ T$ [red line, $V_L(t)$] and its harmonic [green line, $V_1(t)$] and biharmonic [blue line, $V_2(t)$] approximations. (b) Noise difference $S_2 - S_{2,dc}$ for the different waveforms. Dashed lines correspond to zero temperature whereas solid lines correspond to our experimental temperature $k_BT = 0.14\ h\nu$.

harmonic, and $V_2(t) = V_{dc}[1 + \cos(2\pi\nu t) + 0.5\cos(4\pi\nu t)]$ is again the same Lorentzian waveform but truncated to dc and first two harmonics. We show in Fig. 6(b) the numerical difference in the noise, $S_2 - S_{2,dc}$ between ac+dc excitation and dc-only excitation for these three waveforms. At zero temperature (dashed lines), there is a sharp minimum for each integer value of $eV_{dc}/(h\nu)$ for the three waveforms. The Lorentzian reaches zero and the biharmonic is better than the monoharmonic. For $eV_{dc} < h\nu$ the Lorentzian is the worst. At finite temperature (solid lines, $k_BT = 0.14\ h\nu$ as in the experiment), none of the waveforms minimize the noise at quantized values of $eV_{dc}/h\nu$.

[1]L. S. Levitov, H. W. Lee, and G. B. Lesovik, J. Math. Phys. **37**, 4845 (1996).
[2]D. A. Ivanov, H. W. Lee, and L. S. Levitov, Phys. Rev. B **56**, 6839 (1997).
[3]J. Keeling, I. Klich, and L. S. Levitov, Phys. Rev. Lett. **97**, 116403 (2006).
[4]C. Grenier, R. Hervé, E. Bocquillon, F. D. Parmentier, B. Plaçais, J.-M. Berroir, G. Fève, and P. Degiovanni, New J. Phys. **13**, 093007 (2011).
[5]N. d'Ambrumenil and B. Muzykantskii, Phys. Rev. B **71**, 045326 (2005).
[6]M. Vanević, Y. V. Nazarov, and W. Belzig, Phys. Rev. B **78**, 245308 (2008).
[7]M. Vanevic and W. Belzig, Phys. Rev. B **86**, 241306(R) (2012).
[8]G. B. Lesovik and L. S. Levitov, Phys. Rev. Lett. **72**, 538 (1994).
[9]R. J. Schoelkopf, A. A. Kozhevnikov, D. E. Prober, and M. J. Rooks, Phys. Rev. Lett. **80**, 2437 (1998).
[10]L.-H. Reydellet, P. Roche, D. C. Glattli, B. Etienne, and Y. Jin, Phys. Rev. Lett. **90**, 176803 (2003).
[11]J. Gabelli and B. Reulet, Phys. Rev. Lett. **100**, 026601 (2008).

[12]L. Spietz, K. W. Lehnert, I. Siddiqi, and R. J. Schoelkopf, Science **300**, 1929 (2003).
[13]H. Pothier, S. Guéron, Norman O. Birge, D. Esteve, and M. H. Devoret, Phys. Rev. Lett. **79**, 3490 (1997).
[14]F. Pierre, A. Anthore, H. Pothier, C. Urbina, and D. Esteve, Phys. Rev. Lett. **86**, 1078 (2001).
[15]F. Pierre, H. Pothier, P. Joyez, Norman O. Birge, D. Esteve, and M. H. Devoret, Phys. Rev. Lett. **86**, 1590 (2001).
[16]A. Anthore, F. Pierre, H. Pothier, and D. Esteve, Phys. Rev. Lett. **90**, 076806 (2003).
[17]C. Altimiras, H. le Sueur, U. Gennser, A. Cavanna, D. Mailly, and F. Pierre, Nat. Phys. **6**, 34 (2010).
[18]Y. M. Blanter and M. Büttiker, Phys. Rep. **336**, 1 (2000).
[19]P. K. Tien and J. P. Gordon, Phys. Rev. **129**, 647 (1963).
[20]The ac excitation also generates electron-hole correlations. Those are irrelevant for a conductor with small transmission such as our tunnel junction (Ref. 18).
[21]D. M. Berns, M. S. Rudner, S. O. Valenzuela, K. K. Berggren, W. D. Oliver, L. S. Levitov, and T. P. Orlando, Nature (London) **455**, 51 (2008).
[22]J. Bylander, M. S. Rudner, A. V. Shytov, S. O. Valenzuela, D. M. Berns, K. K. Berggren, L. S. Levitov, and W. D. Oliver, Phys. Rev. B **80**, 220506(R) (2009).
[23]M. H. Pedersen and M. Büttiker, Phys. Rev. B **58**, 12993 (1998).
[24]D. M. Berns, W. D. Oliver, S. O. Valenzuela, A. V. Shytov, K. K. Berggren, L. S. Levitov, and T. P. Orlando, Phys. Rev. Lett. **97**, 150502 (2006).
[25]L. S. Levitov (private communication).
[26]E. Akkermans and G. V. Dunne, Phys. Rev. Lett. **108**, 030401 (2012).
[27]F. Chiodi, M. Aprili, and B. Reulet, Phys. Rev. Lett. **103**, 177002 (2009).
[28]J. J. A. Baselmans, A. F. Morpurgo, B. J. Van Wees, and T. M. Klapwijk, Nature (London) **397**, 43 (1999).
[29]D. Prober (private communication).